

## Segregation patterns in binary fluidization

Kamal K. Pandey<sup>1,\*</sup>, Partha S. Goswami<sup>2</sup>, and Manaswita Bose<sup>1</sup>

<sup>1</sup>Department of Energy Science and Engineering, Indian Institute of Technology Bombay, Powai, Mumbai-400076, India

<sup>2</sup>Department of Chemical Engineering, Indian Institute of Technology Bombay, Powai, Mumbai-400076, India

**Abstract.** Segregation mechanism of an initially mixed, size-dispersed binary mixture of particles in a gas-solid fluidized bed has been studied. The non-monotonic mixing/segregation behavior of binary particles with equal mass fraction is explained through variation of mixing indices with time and superficial gas velocities. The study implies that the segregation of particles initiates as the gas flow is introduced. However, beyond a specific gas velocity, the system exhibits remixing of particles in the bed. The pressure drop obtained from the simulations of the packed state of the bed was found to be in agreement with the values predicted by the Kozeny-Carman equation. Two initial states of the bed were used to investigate the segregation during fluidization. First, the fluid was introduced to an initially packed bed. In the second approach, fluid was introduced to the steady state condition of the bed achieved at a lower velocity. Mixing indices were determined using two methods: the entropy-based mixing index and the Lacey mixing index, to assess the macroscopic mixing or segregation within the bed.

### 1 Introduction

Mixing and segregation of polydispersed mixture in a fluidized bed is of interest in industries focusing on coating, drying, and heterogeneous catalytic reactions like fluid bed catalytic cracking [1]. Particles with a large size distribution cause a variety of phenomena in a fluidized bed [2]. Formisani and co-workers [3] have investigated the fluidization behaviour of a bidisperse mixture of different types of particles in gas solid fluidized beds and proposed the expression for the initial and the final fluidization velocities; however, their measurements are predominantly pressure drop based. Vertical and horizontal band formation, partial segregation [4] prior to complete fluidization, are also observed in bi-dispersed fluidized beds. The mixing indices are often used for investigating the mixing and segregation since visualization based experiments are restrictive. Two different methods to determine the mixing indices are mainly used in literature; namely, (a) the Lacey mixing index [5] and (b) the entropy of mixing [6]. While mixing indices provide a macroscopic description of the fluidized bed morphology, the mixing/segregation mechanism requires detailed analysis. One of the methods to perform the analysis is through simulations using the discrete element method; however, performing simulations of a full scale fluidized bed requires simulating a huge number of particles (20-100 million). Simulation of scaled down bed is another possibility; however, the fluidized beds are examples of problems with incomplete dynamic similarity. This highlights the challenges encountered when trying to scale and model fluidized bed systems. [7].

The aim of this work is to determine the mixing indices of bidispersed particles in a scaled-down fluidized bed using CFD-DEM simulations as a first step to provide the mechanism of segregation. The objective also includes to validate the results obtained in the scaled down bed. For validation, a scaled-down fluidized bed is simulated using the CFD-DEM method in the open source software MFiX.

### 2 Methodology

A homogeneous mixture of particles with two different fractions of  $x_{FO} = 0.5$  and  $x_{FO} = 0.1$ , where  $x_{FO}$  is defined as the mass fraction of smaller particles is selected. Simulation runs were conducted in a three dimensional cylindrical bed using particles of equal density ( $2500 \text{ kg/m}^3$ ) and sizes of  $196 \mu\text{m}$  and  $550 \mu\text{m}$  for a wide range of superficial gas velocities. The usual continuum level mass and momentum conservation equations describe the fluid flow. Individual particles are tracked by solving Newton's second law of motion. Inter-particle contact is modeled using a combination of a linear spring, a dashpot, and a slider. The normal spring stiffness constant,  $k_n = 2.6 \times 10^5 \left(\frac{mg}{d}\right)_L$  is used, where the subscript L stands for large particle,  $m$  and  $d$  are mass and diameter, respectively. The ratio of tangential to the normal spring constant is maintained at  $\frac{2}{7}$ . A normal restitution coefficient of 0.9 is selected for both inter-particle and particle-wall collisions. The ratio of the tangential to the normal damping factor is maintained at 0.5.

### 3 Validation

Figure 1 shows the comparison of  $\Delta P/L$  determined using CFD-DEM for three different cases: (1) mono-dispersed

\*e-mail: 214170003@iitb.ac.in

particles with  $d_p = 196\mu\text{m}$  (Case I), (2) a bi-dispersed mixture with 50% by mass of  $d_{p,l} = 550\mu\text{m}$ , and  $d_{p,s} = 196\mu\text{m}$  (Case II,  $x_{FO} = 0.5$ , where  $x_{FO}$  is the mass fraction of the small particles), and (3) with 90% of  $d_{p,l} = 550\mu\text{m}$ , and 10% of  $d_{p,s} = 196\mu\text{m}$  (Case III,  $x_{FO} = 0.1$ ), and compared with that obtained from the Kozeny-Carman equation. A maximum percentage difference of 17%, 10% and 13% was observed for Case I, Case II and Case III, respectively. In addition, the minimum (or initial) fluidization velocity

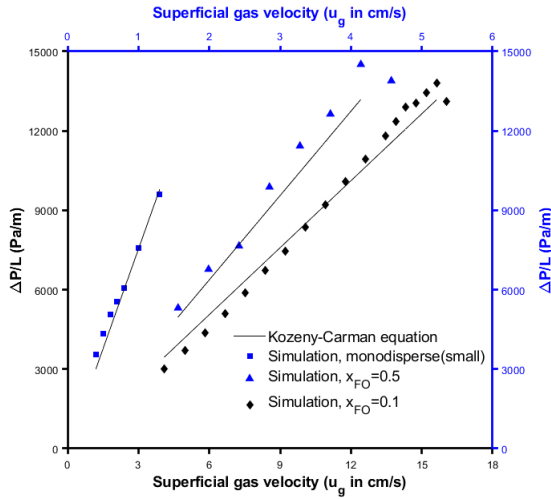


Figure 1: Bed pressure drop

[8] was also compared against the value determined using Eq (1). The difference was found to be less than 10%.

$$u_{if} = \frac{(\rho - \rho_g)\varepsilon_{mf}^3 d_{av}^2}{180\mu_g(1 - \varepsilon_{mf})} g \quad (1)$$

## 4 Results and analysis

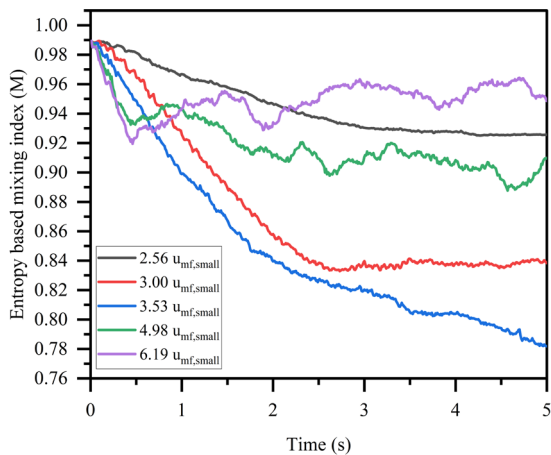


Figure 2: Variation in entropy-based mixing index with time for simulations of a homogeneously mixed bed with  $x_{FO} = 0.5$  at different inlet gas velocities

Figure 2 and Figure 3 show the temporal evolution in entropy based (Eq.2) and Lacey mixing index (Eq.4),

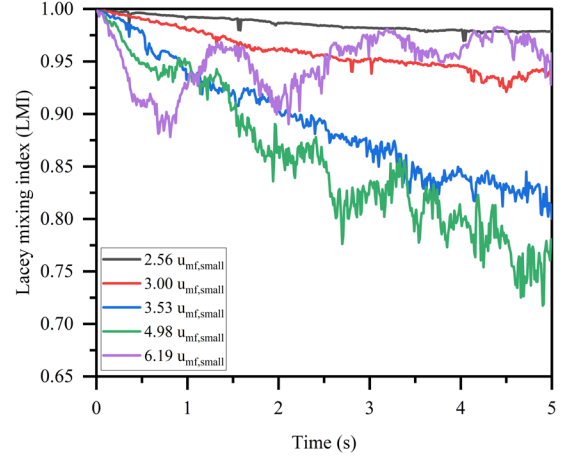


Figure 3: Variation in Lacey mixing index with time for simulations of a homogeneously mixed bed with  $x_{FO} = 0.5$  at different inlet gas velocities

respectively for Case II at five different superficial gas velocities, for which the mixing index based on entropy of mixing [6] is determined as

$$M = \frac{\Lambda}{\Lambda_{mix}} \quad (2)$$

where  $\Lambda$  represents the degree of mixing for a system of a specified number of particles at a particular time step, and  $\Lambda_{mix}$  denotes the degree of mixing for the same number of particles in a thoroughly mixed system. A perfectly mixed system is indicated by  $M = 1$ , while a completely segregated system corresponds to  $M = 0$ . For a binary mixture,  $\Lambda$  is expressed as equation (3) where subscripts  $s$  and  $l$  represent small and large particles, respectively.

$$\Lambda = \sum_N n_N (x_s^N \ln x_s^N + x_l^N \ln x_l^N), \quad (3)$$

This study also uses the Lacey mixing index [5] as the second measure of mixing/segregation, defined as

$$LMI = \frac{s_0^2 - s_r^2}{s_0^2 - s_f^2} \quad (4)$$

where  $s^2$  is the instantaneous concentration variance of a reference type of particle;  $s_r^2$  is the concentration variance for a completely random mixture, and  $s_0^2$  is the concentration variance when in a completely unmixed state.

Both the methods show that, with the increase in superficial gas velocity, the bed reached a state at which the segregation of particles was maximum. With increase in superficial gas velocity beyond this point, the particles began to mix again; however, the superficial gas velocity at which the maximum segregation is observed differs based on the method. Entropy based mixing index suggests the maximum segregation at  $\sim 3.53u_{mf,small}$  and the Lacey mixing index indicates it at  $\sim 4.98u_{mf,small}$ . Mixing indices for Case III are plotted in Figures 4 and 5. Unlike the previous case, the particles tend to segregate with an increase in the superficial gas velocity in this case. Small particles move up and form a layer at the top of the bed.

Figure 6 and 7 illustrates the time variation of flotsam and jetsam volume fraction at different bed heights for Case II,  $x_{FO} = 0.5$  and Case III,  $x_{FO} = 0.1$  respectively. Gas velocities of  $3.53 u_{mf,small}$  in Case II and  $11.42 u_{mf,small}$  in Case III corresponds to the velocity of maximum segregation. It clearly illustrates the axial segregation pattern i.e., the upward movement of the smaller(flotsam) particles, leading to the formation of a distinct layer at the top of the bed.

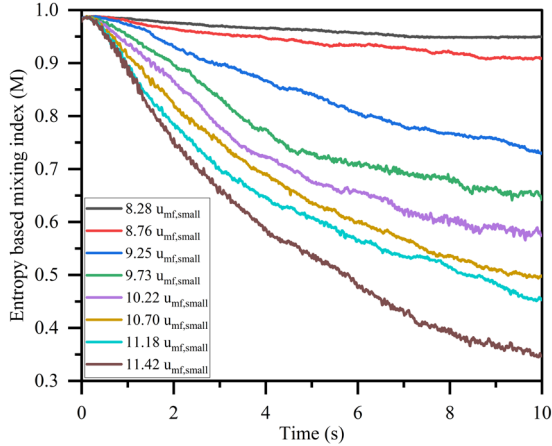


Figure 4: Variation in entropy-based mixing index with time for simulations of a homogeneously mixed bed with  $x_{FO} = 0.1$  at different inlet gas velocities

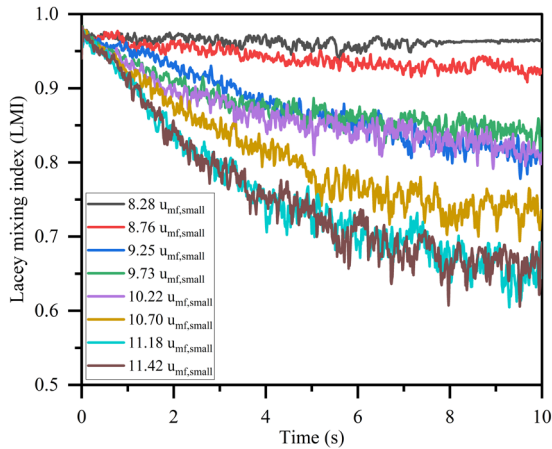


Figure 5: Variation in lacey mixing index with time for simulations of a homogeneously mixed bed with  $x_{FO} = 0.1$  at different inlet gas velocities

This study reveals complex segregation and mixing behavior influenced by varying weight fractions. In Case-II ( $x_{FO} = 0.5$ ), the system exhibits a non-monotonic segregation trend with increasing superficial gas velocity. The bed segregates axially, reaching a maximum degree of segregation at an intermediate gas velocity ( $\sim 3.53 u_{mf,small}$ ). Beyond this threshold, further increases in gas velocity induce significant particle circulation and mixing throughout the bed, even though the superficial velocity remains well below the minimum fluidization velocity of the larger particles.

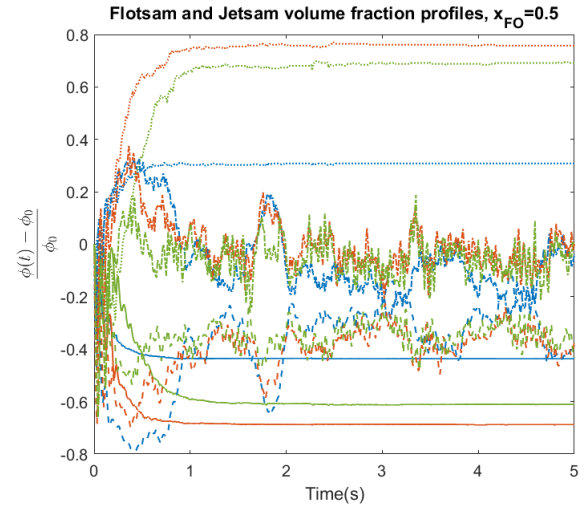


Figure 6: Flotsam and jetsam volume fractions plotted against time at three different bed heights ( $z_1 = 0.5$  mm, blue;  $z_2 = 1.5$  mm, red;  $z_3 = 2.5$  mm, green) for a binary mixture with  $x_{FO} = 0.5$ . Results are shown for two gas velocities:  $v_1 = 3.53 u_{mf,small}$  ( $0.42 u_{mf,large}$ ) and  $v_2 = 6.19 u_{mf,small}$  ( $0.74 u_{mf,large}$ ). Flotsam volume fractions are represented by **solid lines**(-) ( $v_1$ ) and **dashed lines**(-) ( $v_2$ ), while jetsam volume fractions are represented by **dotted lines**(:) ( $v_1$ ) and **dash-dot lines**(-) ( $v_2$ ).

This counterintuitive observation in Case-II can be attributed to interparticle momentum transfer between the two phases. Finer particles, due to their substantially lower minimum fluidization velocity and higher number density, fluidize earlier and contribute to bed expansion. This expansion leads to a localized increase in voidage and interstitial gas velocity, which, in turn, facilitates the motion of the coarser particles through enhanced drag and bubble-induced lifting forces. Consequently, the system undergoes induced fluidization, wherein the fine particles dynamically assist the onset of motion and circulation of the coarse particles, even when the gas velocity is subcritical for fluidization of the coarse phase.

In case-III, when the mixture has mostly large particles and only about 10% smaller particles (by mass), the simulations show that the particles stay segregated. In this case, there aren't enough small particles to influence the motion of the larger particles. So, the behavior of the bed is mostly controlled by how the large particles fluidize. The small particles, which fluidize earlier, get carried upward and accumulate near the top of the bed.

In the previous cases, simulations were initiated with the same initial condition. An alternative approach was also followed for a binary mixture with  $x_{FO} = 0.1$ , in which the gas velocity was successively increased. The obtained initial fluidization velocity was found to be the same for both approaches.

Figure 8 plots the steady state values of the mixing indices as a function of the superficial gas velocities for Case II and Case III. A distinct minima is observed for Case II (binary mixture with 50% mass fraction); however,

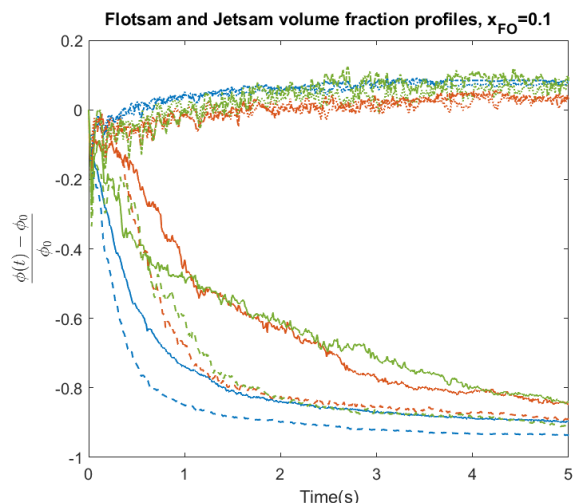


Figure 7: Flotsam and jetsam volume fractions plotted against time at three different bed heights ( $z_1 = 0.5$  mm, blue;  $z_2 = 1.5$  mm, red;  $z_3 = 2.5$  mm, green) for a binary mixture with  $x_{FO} = 0.1$ . Results are shown for two gas velocities:  $v_1 = 10.70 u_{mf,small} (1.27 u_{mf,large})$  and  $v_2 = 11.42 u_{mf,small} (1.35 u_{mf,large})$ . Flotsam volume fractions are represented by **solid lines(-)** ( $v_1$ ) and **dashed lines(- -)** ( $v_2$ ), while jetsam volume fractions are represented by **dotted lines(:)** ( $v_1$ ) and **dash-dot lines(-.)** ( $v_2$ ).

the mixing indices decreases monotonically with superficial gas velocity for Case III ( $x_{FO} = 0.1$ ).

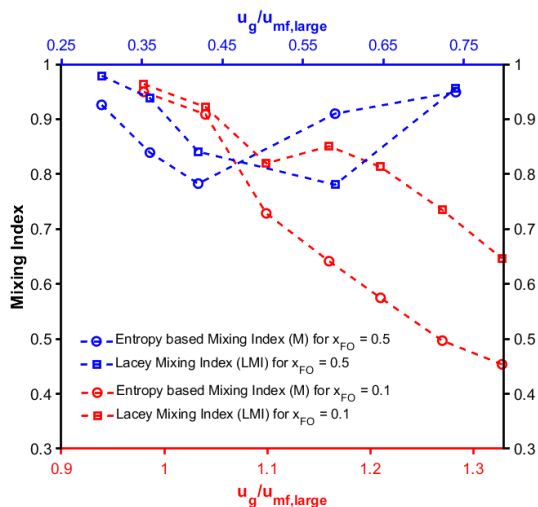


Figure 8: Variation in mixing index with superficial gas velocity for  $x_{FO} = 0.5$  and  $x_{FO} = 0.1$  using two different mixing indices

## 5 Conclusion

This study investigates the segregation behavior of a size-dispersed binary mixture of particles in a gas-solid fluidized bed. Segregation in a binary system of particles was studied using mixing indices. The following are the key conclusions of this work:

- For a binary mixture with  $x_{FO} = 0.5$ , the non-monotonic mixing/segregation behavior of particles was observed. As the superficial gas velocity increased, the bed reached a state at which the segregation of particles was at its maximum. With a further increase in superficial gas velocity beyond this point, the particles began to mix again.
- For a binary mixture with  $x_{FO} = 0.1$ , the particles tended to segregate axially with the increase in superficial gas velocity. Accumulation of flotsam particles in the top quarter of the bed was observed. As the time progressed, flotsam particles that were initially caged within the interstitial space between the layer of the jetsam particles, came out of it and reached the top of the bed.
- For a binary mixture with  $x_{FO} = 0.1$ , a different set of simulations was also performed, in which the gas velocity was successively increased. The initial fluidization velocity was found to be the same for both methods. The segregation of particles also showed a similar trend.

## References

- [1] Zhu, H., Lettieri, P., Materazzi, M., Systematic analysis of mixing and segregation patterns of binary mixtures in fluidised beds for multi-functional processes. *Powder Technology* **449**, (2025) <https://doi.org/10.1016/j.powtec.2024.120419>
- [2] Beetstra, R., Nijenhuis, J., Ellis, N., van Ommen, J. R., The influence of the particle size distribution on fluidized bed hydrodynamics using high-throughput experimentation. *AICHE journal*, **55(8)**, 2013-2023(2009). <https://doi.org/10.1002/aic.11790>
- [3] Formisani, B., Girimonte, R., Longo, T., The fluidization process of binary mixtures of solids: Development of the approach based on the fluidization velocity interval. *Powder Technology*, **185(2)**, 97-108 (2008). <https://doi.org/10.1016/j.powtec.2007.10.003>
- [4] Gilbertson M.A., Eames I., Segregation patterns in gas-fluidized systems. *Journal of Fluid Mechanics* **433**, 347-356 (2001). <https://doi.org/10.1017/S0022112001003950>
- [5] P. M. C. Lacey, Developments in the theory of particle mixing. *Journal of applied chemistry* **4(5)**, 257-268 (1954). <https://doi.org/10.1002/jctb.5010040504>
- [6] B. Remy, J. G. Khinast, B. J. Glasser, Polydisperse granular flows in a bladed mixer: Experiments and simulations of cohesionless spheres. *Chemical Engineering Science* **66(9)**, 1811-1824 (2011). <https://doi.org/10.1016/j.ces.2010.12.022>
- [7] Sanderson, J., Rhodes, M., Bubbling fluidized bed scaling laws: Evaluation at large scales. *AICHE journal*, **51(10)**, 2686-2694 (2005). <https://doi.org/10.1002/aic.10511>
- [8] B. Formisani, R. Girimonte, and V. Vivacqua, Fluidization of Mixtures of Two Solids Differing in Density or Size. *AICHE Journal* **57(9)**, 2325-2333 (2011). <https://doi.org/10.1002/aic.12450>